Quantification of anomalous behaviour in Rayleigh velocity dispersion curves of stiffening and loading layer/substrate configurations

ABDENOUR HADDAD*
Laboratoires des Semi-Conducteurs, Département de Physique, Faculté des Sciences, Université Badji Mokhtar, BP 12, Annaba, DZ-23000, Algerie
Département des Sciences Exactes et Informatique, École Normale Supérieure de Constantine, DZ-25000, Algerie

The determination and the understanding of the phenomena of elasticity in thin films are indispensable for the design and technology of various modern components. In this context, layer stiffening effects and mass loading effects are studied for several layer/substrate configurations via positive and negative dispersion curves respectively. The investigated structures showed four types of anomalies; a peak resulted of velocities greater than the Rayleigh velocity of the substrate, and a valley which is resulted of velocities smaller than the Rayleigh velocity of the layer, in the case of structures having $1>V_{TL}/V_{TS}>1/\sqrt{2}$, as well as the inverse phenomenon, i.e. a valley comes from velocities smaller than the Rayleigh velocity of the substrate, and a peak obtained from velocities greater than the Rayleigh velocity of the layer, in the case of structures which having $V_{TL}/V_{TS}>1$. The anomalous behaviours appeared in the dispersion curves of Rayleigh velocity are studied in terms of the extreme velocity, V_{Ext}, which represents the maximum value of the peak, V_{Max}, and the minimum value of the valley, V_{Min}. The appearance and disappearance of any type of these phenomena is analysed and quantified in terms of a combined elastic parameter (δ). A general relationship which quantifies the extreme velocities in both cases, was deduced.

(Received October 2, 2012; accepted February 20, 2013)

Keywords: Elastic properties, Thin films, Surface acoustic waves, Anomalous, Stiffening effect, Loading effect

1. Introduction

In quantitative microscopy, the investigation of combination layer/substrate gives a great deal to calculate a lot of parameters as densities, attenuation, thickness, adhesion and elastic modulus….etc. But the most important one is the simulation of velocities specially that of Rayleigh. In system layer/substrate, Rayleigh velocity as all velocities of known modes becomes dispersive. It changes its value as a function of thickness if all other parameters considered being constants [1-3]. In this case, two classes of dispersion can be observed depending on the ratio of transverse wave velocities of the film, V_{TL}, and of the substrate, V_{TS}. When transverse wave velocity is greater than that of the substrate, the phase velocity increases; it is said that the layer stiffens the substrate [4-6]. On the other hand, a film whose transverse wave velocity is less than that of the substrate, the phase velocity decreases with thickness; the film is said to load the substrate [7–9]. In this context we have focused our research on structures characterizing by a slope which is similar to the mass loading effect curves as well as the structures verifying stiffening effect for $0<\delta<4$, where δ equals to the densities ratio divided in Rayleigh velocities ratio of system layer/substrate, $\delta=(\rho_L/\rho_S)/(V_{RL}/V_{RS})$ [10]. Such parameter is used to predict the kind of anomalous behaviours appears in Rayleigh velocity dispersion curves and to quantify the extreme velocities in these phenomena. To do this, we have simulated theoretically more than 30 combinations using Sheppard and Wilson model.

2. Computing method

In this investigation we carried out calculations using spectral methods whose details could be found elsewhere [11-13]; it permits the calculation of acoustic materials signatures, $V(z)$, which given by the expression [13]:

$$V(z)=\int_0^{\theta_m} P^2(\theta)R(\theta)\exp(2ik_0Z\cos\theta)\sin\theta\cos\theta d\theta \quad (1)$$

where $P(\theta)$ is the lens pupil function, θ_m is the half-aperture angle of the lens, z is the defocusing distance

and $k_0 = 2\pi / \lambda$ is the wave number in the coupling liquid, $j = \sqrt{-1}$ and the reflection coefficient, $R(\theta)$, which given by expression [2]:

$$R(\theta) = \frac{Z_L \cos^2 2\theta_T + Z_T \sin^2 \theta_T - \rho_{liq} V_{liq} / \cos\theta}{Z_L \cos^2 2\theta_T + Z_T \sin^2 \theta_T + \rho_{liq} V_{liq} / \cos\theta} \quad (2)$$

where: Z_L, Z_T, ρ_{liq} and V_{liq} are longitudinal impedance, transverse impedance, coupling liquid density and the propagating wave velocity in the liquid, respectively.

The deduced acoustic materials signatures signals have to be corrected to eliminate the lens response, $V_l(z)$, that is equivalent to the response of gold as a perfect reflecting material [12] by subtracting the response of the lens $V_l(z)$ from V(z) to obtain the real signal of the sample which is characterized by a periodic oscillation due to constructive and destructive interferences. Thus, its analysis can be performed via Fast Fourier Transform, FFT, [16] from which the Rayleigh velocity can be determined [11, 17] using the well-known relationship [18].

$$V_R = V_{liq} / [1 - (1 - V_{liq} / 2f\,\Delta z)^2]^{1/2} \quad (3)$$

where V_{liq} is the speed of sound in liquid, f is the frequency, and Δz is the period of the oscillation of the $V(z)$ curve.

Calculations were carried out using standard operating conditions of conventional scanning acoustic microscope (operating frequency, $f = 142$ MHz, half-opening angle of the lens $\theta_m = 50°$ and water as coupling liquid).

3. Results and discussions

3.1. Dispersion of Rayleigh waves velocity

It is worth noting that there exist two types of dispersion curves of Rayleigh waves due to either stiffening effect (positive dispersion curves) or mass loading effect (negative dispersion curves). In the Stiffening effect**,** when shear wave velocity of the layer, V_{TL}, is greater than that of the substrate, V_{TS}, the phase velocity of Rayleigh waves increases from the substrate velocity to that of the layer, as displayed by curve (a) in Fig. 1. The Loading effect is the inverse phenomenon, as shown by curve (b) in Fig. 1. Thus, if the shear wave velocity of the substrate is greater than that of the layer, the phase velocity of Rayleigh wave's decreases [14, 15]. Conventionally, the velocity increases/decreases from that of the substrate, V_{RS}, at a normalized layer thickness $e / \lambda_T = 0$, where e is the layer thickness and λ_T is the wavelength of the transverse waves propagating in the layer, then the velocity saturates when it approaches asymptotically a value that corresponds to the Rayleigh velocity of the layer, V_{RL}, at a specific normalized thickness for each combination[13].

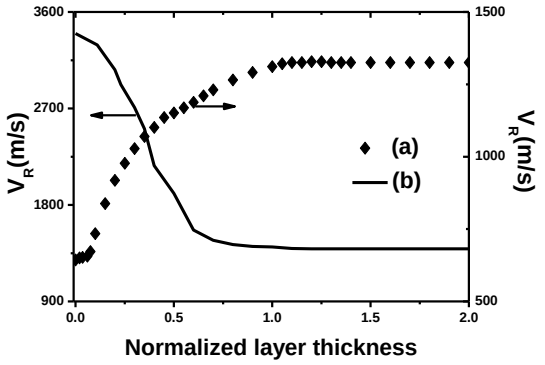

Fig. 1. Types of Rayleigh velocity dispersions (a) Positive dispersion for Anthracene/Teflon (b) Negative dispersion for Anthracene/SiO_2 substrate [15].

3.2. Anomalous behaviour in curves with loading effect

The obtained results showed that the mass loading effect appears with abnormal dispersion in the ranges of the elastic parameter δ; $0.3 < \delta < 1.2$ and $3.1 < \delta < 4$. In the first range, the velocity takes values superior to that of the substrate. Whereas, in the second range the velocity takes values inferior to that of the layer velocity. In both cases, the velocity reaches an extreme value (V_{Ext}). The anomalous behaviour presented an extreme velocity ($V_{Ext} = V_{Max}$), which is greater than Rayleigh velocity in the substrate, V_{RS}, and an extreme velocity ($V_{Ext} = V_{Min}$) smaller than Rayleigh velocity in the layer, V_{RL}, as shown in Fig. 2 by curves (a) and (b) respectively.

The analysis of the results obtained for different combinations led to notice the existence of negative dispersion which is associated with the mass loading effect. Whereas, the curve (a) in Fig. 2 shows that, unlike conventionally, for small thickness the velocity increases to reach a maximal value of phase velocity (V_{Max}) greater than that of the substrate (peak anomaly) before it decreases sharply to approach asymptotically the Rayleigh velocity of the layer, for a large normalized layer thickness. On the other hand, curve (b) in Fig. 2 illustrates the anomaly which is resulted from the decreasing of the phase velocity starting from the substrate velocity to reach a minimal value (V_{Min}) less than that of the layer before it increases to reach the layer velocity at a saturation's thickness.

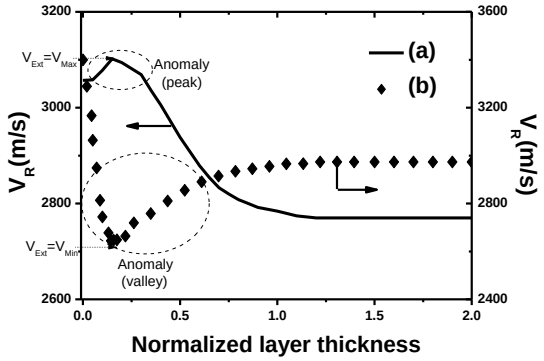

Fig. 2. Anomalous behaviour in negative velocity dispersion curves for (a) ZnO/Steel ($\delta = 0.79$) and (b) Iron(soft)/Q ($\delta = 3.99$).

3.3. Anomalous behaviour in curves with stiffening effect

The obtained results show clearly that for the elastic parameter δ ranges; $0 < \delta < 0.3$ and $1.2 < \delta < 3.1$, the stiffening effect (or positive dispersion curves of Rayleigh velocity) appears with abnormal dispersion in both ranges. In the former, the velocity takes values superior to that of the layer to reach an extreme value ($V_{Ext} = V_{Max}$). Then, it decreases to saturate at layer velocity, V_{RL}, as it is shown by curve (a) in Fig. 3. However, in the latter, the velocity takes values inferior to that of substrate's velocity to reach an extreme value ($V_{Ext} = V_{Min}$). After that, it increases to reach V_{RL} when it saturates, as it is shown by curve (b) in Fig. 3.

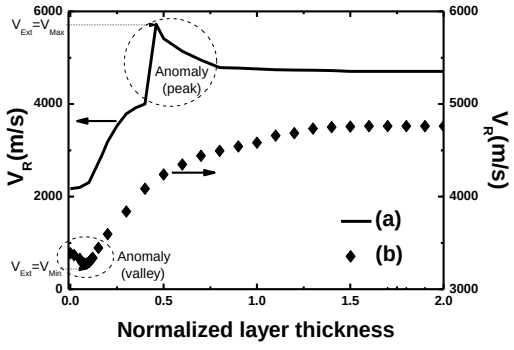

Fig. 3. Anomalous behaviour in positive velocity dispersion curves for (a) Si/Cu($\delta = 1.12$) and (b) TiC/Q ($\delta = 1.70$).

3.4. Quantification of anomalous behaviour

To enrich this investigation and to confirm the anomalous behaviours, as well as to quantify the existence of these anomalous phenomena observed in the structures characterized by the elastic parameter, δ, whose values were varied, from 0.1146 to 3.9918; we have simulated several combinations with different densities whose range from 1250 kg/m^3 to 15000 kg/m^3 and a ratio of transverse velocities range $0.759 \le V_{TL}/V_{TS} \le 3.289$.

To compare the whole results obtained for different combinations, we have plotted in Fig. 4 the extreme velocity (V_{Ext} which represents both V_{Max} and V_{Min}) as function of a dimensionless elastic parameter ζ. Where, ζ equals to δ multiplied by the normalized layer thickness at which the velocity reaches the extreme value ($\zeta = \delta \times (e/\lambda_T)_{Ext}$). The obtained results show an exponential decay which can be expressed via curve fitting (solid line in figure 4) as follows:

$$V_{Ext} = 52000 \exp[-\zeta / 0.019] + 2700 \qquad (4)$$

The importance of this formula lies in their simplicity and generality. This formula can be used to determine and to predict not only the existence of several types of dispersion but also the onset of the anomalous behaviour by just knowing the elastic parameter δ.

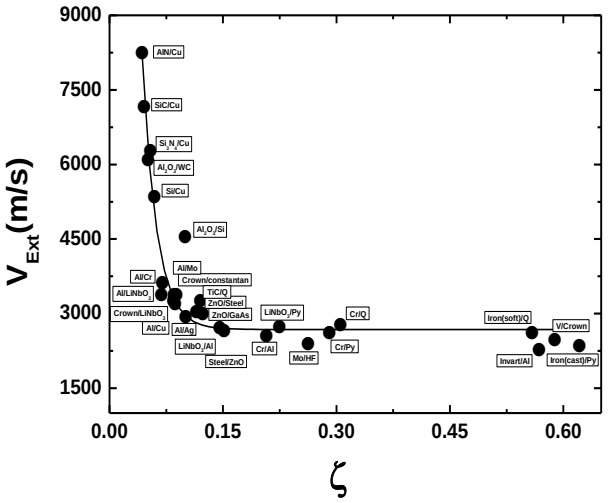

Fig. 4. Effects of normalized layer thickness and elastic parameter δ on extreme velocity; solid dots represent the calculated results and solid line is the fitting curve.

4. Conclusion

Anomalous behaviour, obtained in velocity dispersion curves, was found to be occurred only for $V_{TL}/V_{TS} > 1/\sqrt{2}$. Using the parameter $\delta = (\rho_L/\rho_S)/(V_{RL}/V_{RS})$ enabled us to conclude that in velocity dispersion curves of mass loading effect; the phenomenon (velocity higher than the substrate V_R), occurs for $0.3 < \delta < 1.2$ while, the inverse anomalous behaviour (velocity lower than the layer V_R) appears for $3.1 < \delta < 4$. In contrast, in the dispersion curves of

stiffening layers; the phenomenon (velocity greater than the layer V_R) occurs for $0<\delta<0.3$. However, for $1.2<\delta<3.1$ the anomalous behaviour (velocity smaller than the substrate V_R) dominates. Furthermore, we were able to determine simple formula, relating maximal and minimal velocities of the peaks and valleys observed abnormally in these curves of the form: $V_{Ext} = 52000 \exp[-\zeta / 0.019] + 2700$. Such formula can be used to predict and to quantify the anomalous behaviour.

Acknowledgements

This work was carried out at the « Laboratoire des Semi-Conducteur, Département de Physique, Faculté des Sciences, Université Badji Mokhtar, Annaba, Algérie ». In addition the author would like to thank Professor A. Doghmane for helpful discussions and Professor Z. Hadjoub for the provision of computer code and laboratory facilities.

References

[1] P. V. Zinin, in Handbook of Elastic Properties of Solids, Liquids and Gases, eds. Levy, Bass and Stern, Academic Press, New York, 187, 2001.
[2] A. Briggs (2ed ed.), Acoustic Microscopy. Oxford: Clarendon Press; 2010.
[3] S. Bouhedja, I. Hadjoub, A. Doghmane, Z. Hadjoub, Phys Stat Solid (a); **202**(6), 1025 (2005).
[4] H. F. Tiersten, J. Appl. Phys. **40**, 770 (1969).
[5] W. S. Ohm, M. F. Hamilton, J Acoust Soc Am; **115**(6), 2798 (2004).
[6] I. Beldi, Z. Hadjoub, A. Doghmane, 5th World Congress on Ultrasonic, Paris; 777 (2003).
[7] Z. Hadjoub, I. Beldi, M. Bouloudnine, A. Gacem, A. Doghmane, Elec Lett IEE; **34**(3), 313 (1998).
[8] J. D. Achenbach, Ultrasonics **40**, 1 (2002).
[9] Z. Guo, J. D. Achenbach, A. Madan, K. Martin, M. E. Graham, Thin Solid Films; **394**, 189 (2001).
[10] Z. Hadjoub, I. Beldi, A. Doghmane, CR Phys; **8**, 948 (2007).
[11] J. Kushibiki, N. Chibachi, IEEE Transonic Ultrason; SU-**32**, 189 (1985).
[12] A. Doghmane, Z. Hadjoub, J Acoust Soc Am; **92**, 1545 (1992).
[13] C. G. R. Sheppard, Wilson T. Appl Phys Lett. **38**, 858 (1981).
[14] A. Haddad, M. Doghmane, Z. Hadjoub, A. Doghmane, J. Optoelectron. Adv. Mater.- Symposia; **1**, 285 (2009).
[15] P. Zinin, M. H. Manghnani, S. Tkachev, V. Askarpour, Phys Rev B; **60**(4), 2844 (1999).
[16] W. Li, J. Achenbach, J Acoust Soc Am; **100**, 1529 (1996).
[17] Y. Ohashi, J. Kushibiki, IEEE Trans Ultrasonics Ferroelectr Freq Control; **51**, 686 (2004).
[18] W. Parmon, H. L. Bertoni. Electon Lett; **15**, 684 (1979).

*Corresponding author: ab_haddad@yahoo.fr